THE BULLETIN OF OKAYAMA UNIVERSITY OF SCIENCE No. 42 A pp. 53-61 (2006)

Difference in Temperature-Humidity Index between Commercial and Residential Spaces in Okayama City, Western Japan

—Relationship between Sea Breeze and Thermal/Humidity Environments—

Yukitaka OHASHI, Tomokazu KAWABE, Hiroyuki KUSAKA*,
Yujiro HIRANO**, Hironori FUDEYASU*** and Kazuhito FUKAO****

Department of Biosphere-Geosphere System Science, Faculty of Informatics, Okayama University of Science, 1-1 Ridaicho, Okayama 700-0005, Japan

* *Center for Computational Sciences, University of Tsukuba, Japan*

** *Faculty of Engineering, Gunma University, Japan*

*** *Japan Agency for Marine-Earth Science and Technology, Japan*

**** *Faculty of Engineering, Gifu University, Japan*

(Received September 11, 2006; accepted November 6, 2006)

We observed the meteorological elements to understand the thermal environment in human living spaces. Our research focused on commercial and residential building types in Okayama City, Western Japan. Measured temperature-humidity indices (THI) in the commercial space were 0.8−1.4 higher than THI in the residential space for 17−19 JST. These difference were considered statistically significant, which caused noticeable discomfort for occupants of the commercial spaces. For instance, at 19 JST, the THIs of the commercial and residential spaces were 75.9 and 74.5, respectively. At 18−19 JST, the relative humidity in the commercial space was still 10 % higher than that of the residential space, even though both building types had the same air-temperature. This indicates that the commercial space retains high specific humidity longer than residential space. When the sea breeze arrived, the specific humidity at the commercial space increased rapidly in most observation sites. The specific humidity in the residential space decreased until the evening. The differences were caused by the moist air traveling from a river about one kilometer away from the commercial space. This moist air increases the THI and enhances a risk of the heat disorder in the commercial space.

Keywords: commercial and residential spaces; temperature-humidity index; meteorological observation; sea breeze

1. Introduction

The heat indices, such as temperature-humidity index (THI) and effective temperature (ET), are used to evaluate a comfort of the urban park (Barradas 1991; Saaroni and Viz 2003), livestock stress (Casa and Ravelo 2003; Somparn et al. 2004), and the heat stress in outdoor activities (Hoshi and Inaba 2005). In Japan, the urban heat island phenomenon, caused by the artificial land surfaces and anthropogenic heat release, has been a serious social problem. This is because many patients of the heat disorder occur in urban areas during summer season. It is considered that the heat index is useful to avoid a risk of the heat disorder. Therefore, to evaluate the heat index in the urban area is important for avoiding a risk of the heat disorder. Since the urban area, however, includes various land-use spaces, it is

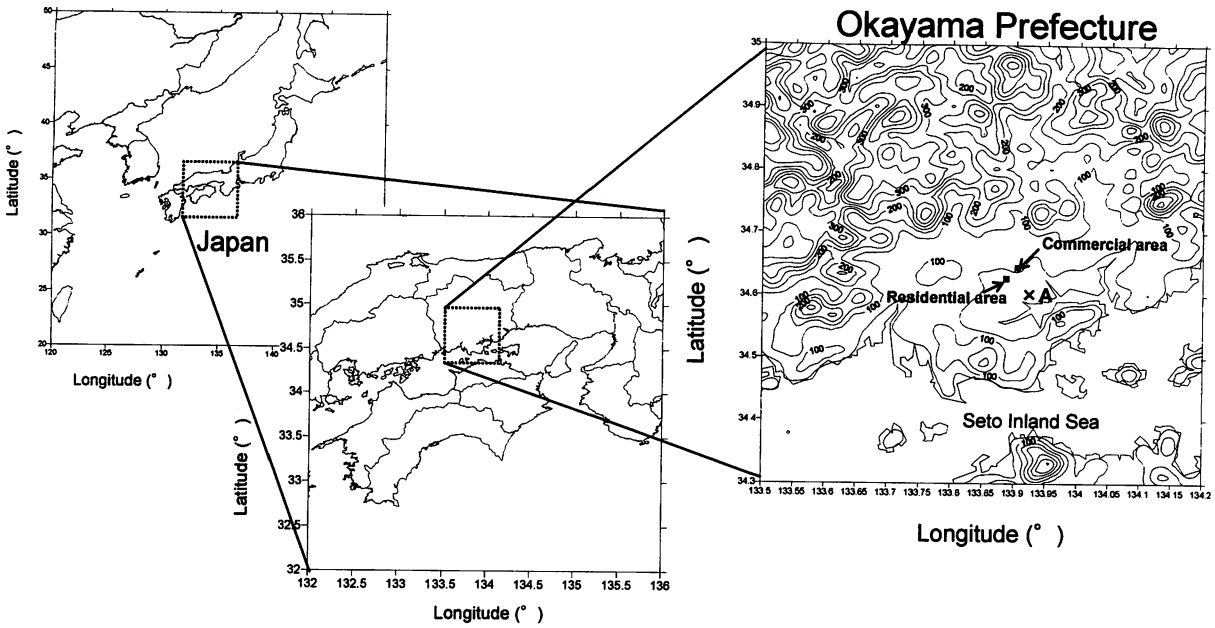

Fig.1 Map showing the location of Okayama City in Western Japan.

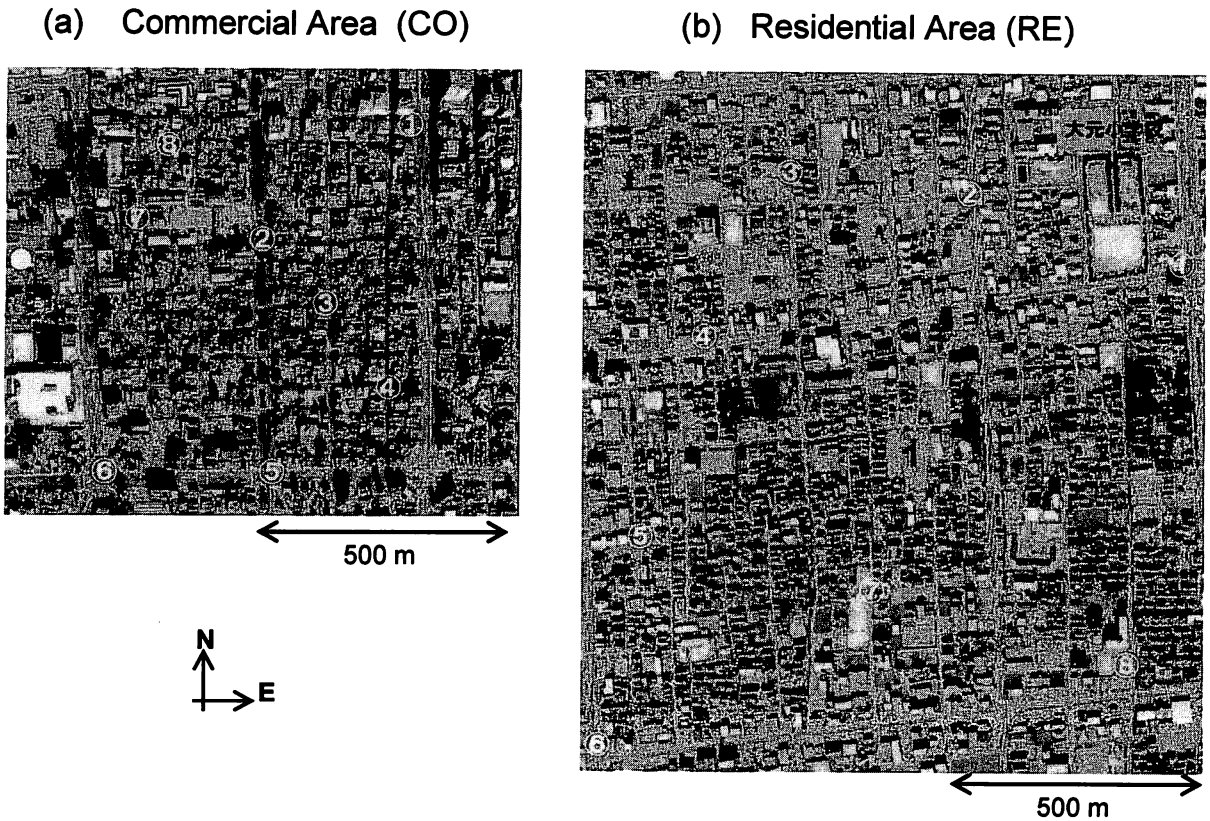

Fig.2 Aerial photographs of study area: a) commercial and b) residential spaces in Okayama City. Numerals represent the observation sites. The solid circle in Fig.2a indicates the Okayama Meteorological Observatory.

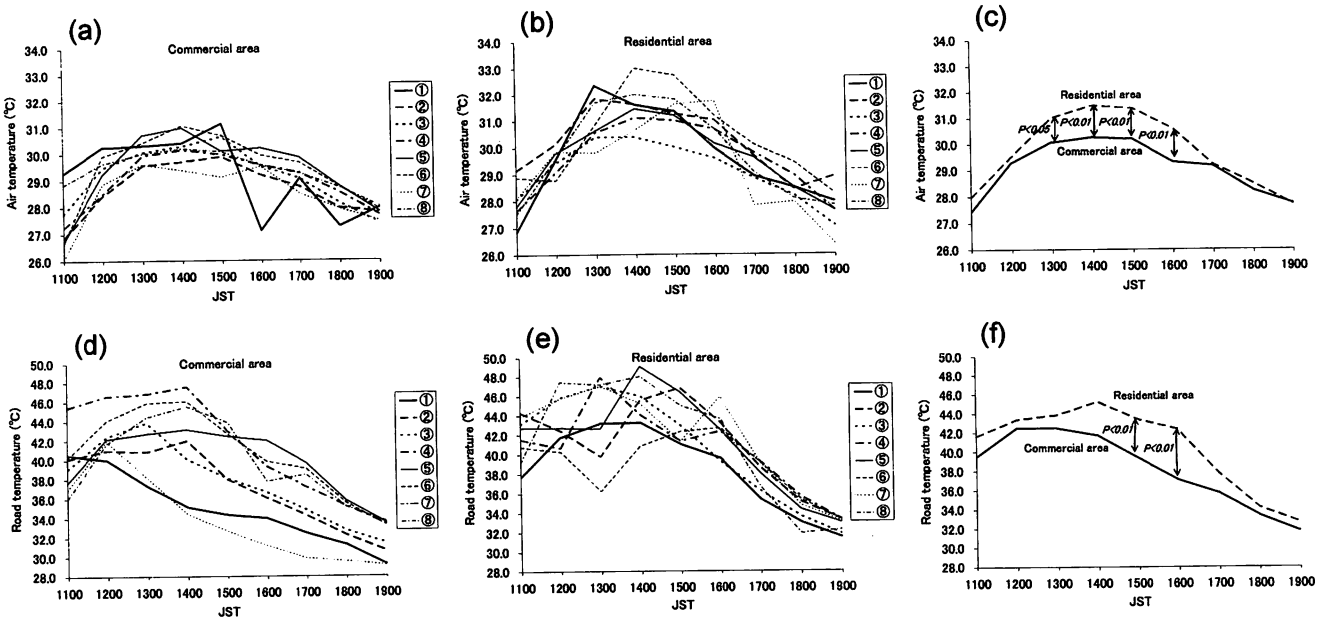

Fig. 3 Temporal variations of (a) (b) (c) air temperature and (d) (e) (f) road temperature measured at the eight observation sites as shown in Fig. 2. The left and central panels represent the commercial and residential spaces, respectively. The right panels are spatially-averaged air and road temperatures.

required to clarify the difference in the heat index among the land-use spaces. Accordingly, we will report the difference in the temperature-humidity index between commercial and residential spaces of a middle scale city, Okayama in Western Japan. The temperature-humidity index will be calculated from the meteorological elements, observed by the authors and their colleague, in the urban area and surrounding.

The artificial land surfaces generally cause the air to dry in the urban area (Aida and Yaji 1979; Oke 1988; Givoni 1991; Lemonsu and Masson 2002), which will reduce a risk of the heat disorder. However, our observation shows that an urban area (commercial space) in Okayama is more humid than a surrounding area (residential space) from the afternoon. The urban humid conditions remain till the evening in spite of the same air-temperature between the two areas. This causes a discomfort environment and a risk of the heat disorder to continue for a long time in the urban area. In this paper, we will discuss a mechanism that produces the above findings.

2. Observation

Our investigation was made for 1000－2000 JST on September 3, 2004 at the commercial space with the multi-storied office buildings and huge human activities, and the residential space with one and two-storied housings in Okayama city (Fig. 1). We hereinafter call the commercial and residential spaces the CO and RE, respectively. We measured the dry-bulb and wet-bulb temperatures, wind speed and direction, road-surface temperature as the surface meteorological elements, at eight locations in each spaces. The observation domain in the CO extends over 500-m square, while the domain in the RE does over 800-m square. The observation sites were chosen so as to include north-south streets, east-west streets, and crossings (Fig. 2), and we passed the sites once an hour by bicycle to measure the meteorological elements. While the sky view factors of 0.4－0.6 mainly appear in the CO, those of 0.7－0.8 in the RE appear. The observation spaces are located at about 16 km away from the south coast of the Seto Inland Sea. The RE is located about 1.5 km southeastward from the CO.

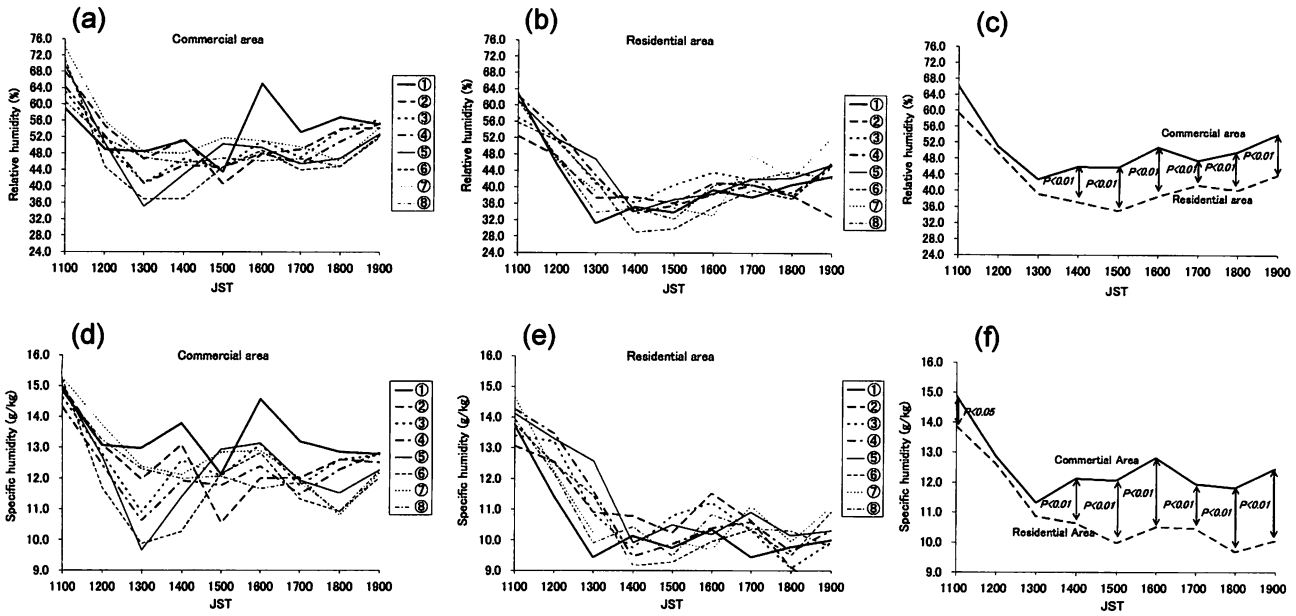

Fig. 4 Same as Fig. 3 but for (a) (b) (c) relative humidity and (d) (e) (f) specific humidity.

Since the Japan Island was covered with the Pacific high pressure during the observation period, the weather in Okayama City was clear sky and calm conditions. In the morning hours, the north wind of 1−2 m s^{-1} in speed was recorded at the Okayama Meteorological Observatory (Fig. 2a). On the other hand, the afternoon wind of 3−4 m s^{-1} in speed blew from the south-east direction. The air temperature reached nearly 30 ℃ in the early afternoon. The daytime wind data showed that the wind speed sharply increased after 1310−1320 JST and then reached the maximum value at 1350−1400 JST. The air temperature measured at this time showed the rapid decrease of nearly 1.0 ℃ between 1340 JST and 1350 JST; no shade effects of clouds on the air temperature appear, from the analysis of the sunshine duration data.

3. Results

Figures 3 and 4 show the measured meteorological elements— air temperature (dry-bulb temperature), road temperature, relative humidity, specific humidity. The specific humidity was calculated from the dry- and wet-bulb temperatures measured by our observation, and the air pressure measured at the Okayama Meteorological Observatory. The air temperatures measured in the CO are entirely lower than those in the RE (Figs. 3a and 3b). A spatially-averaged air temperature in the CO is 1.2 ℃ lower than that in the RE for 1400−1600 JST at $P < 0.01$. For instance, at 15 JST, 30.2 ℃ and 31.4 ℃ were recorded for the CO and RE, respectively. Although the air-temperature increases in the CO stop at 1300 JST, most of air-temperatures in the RE increase till 1400 JST. Also, the spatially-averaged road temperature (Fig. 3f) in the CO is 3.5−5.3 ℃ lower than that in the RE during the same period (with $P < 0.01$ at 1500 JST and 1600 JST). In the morning and evening hours, however, the air and road temperatures are slightly different between the CO and RE.

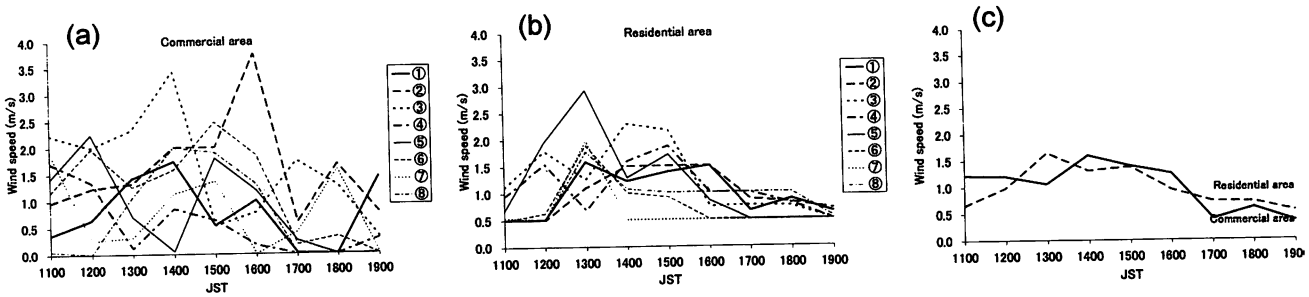

Fig. 5 Same as Fig. 3 but for (a) (b) (c) wind speed.

As can be seen in Fig. 4c, a spatially-averaged relative humidity in the CO is 9−12 % higher than that in the RE for 1400−1600 JST at $P < 0.01$. For instance, at 1500 JST, 45.8 % and 35.0 % were recorded for the CO and RE, respectively. Moreover, the relative humidity in the CO is 10 % higher than that in the RE at 1800−1900 JST also with $P < 0.01$. For instance, at 1900 JST, 54 % and 44 % were recorded for the CO and RE. These features are not only attributed to the difference of air-temperature but also the difference of water-vapor content. At 1500 JST, the relative humidity in the CO is 10.8 % higher than that in the RE; 8.3 % of 10.8 % is due to the water vapor increasing, while the remaining 2.5 % is due to the air-temperature decreasing. At 1900 JST, the relative humidity in the CO is 10.0 % higher than that in the RE; all of 10.0 % is due to the water-vapor increasing, because the values of air temperature are the same between the CO and RE. In fact, a spatially-averaged specific humidity in the CO gradually increases after 1300 JST, whereas that in the RE decreases continuously (Fig. 4f).

The wind speeds measured in the CO and RE are shown in Fig. 5. In the CO, the magnitudes of wind speed widely vary with the sites; the extremely weak and extremely strong winds are measured at the same time (Fig. 5a). In the RE, such a spatial variation of wind speed is not measured throughout the observations (Fig. 5b). A spatially-averaged wind speeds are, however, almost the same between the CO and RE (Fig. 5c).

We calculated the THI using the following relation:

$$\mathrm{THI} = 0.81T + 0.01RH(0.99T - 14.3) + 46.3 \quad (1)$$

where T is the air temperature and RH the relative humidity. This THI proposed by National Astronomical Observatory (2004) is adopted for Japanese discomfort index. As can be seen in Fig. 6c, a spatially-averaged THI in the CO is 0.8−1.4 higher than that in the RE for 1700−1900 JST (with $P < 0.05$ at 1700 JST, and $P < 0.01$ at 1800−1900 JST). For instance, at 1900 JST, 75.9 and 74.5 were recorded for the CO and RE, respectively. At other times, the THI in the CO is almost the same as that in the RE. This is because there is little different in temperature between both spaces despite that the larger absolute humidity is kept in the CO.

The THI is a heat index without influence of wind effects. Accordingly, we also calculated the ET in the both spaces (Figs. 6d−6f) from the effective temperature chart. A spatially-averaged ET in the CO is 0.5−0.9 ℃ higher than that in the RE (with $P < 0.05$ at 1700 JST and $P < 0.01$ at 1900 JST). For instance, at 1900 JST, 23.8 and 22.9 were recorded for the CO and RE, respectively. Similarly with the THI, there is no difference in ETs between the CO and RE until the evening (except 1100 JST). This is caused by the fact that the spatially-averaged wind speeds are slightly different between CO and RE, as can be seen in Fig. 5c.

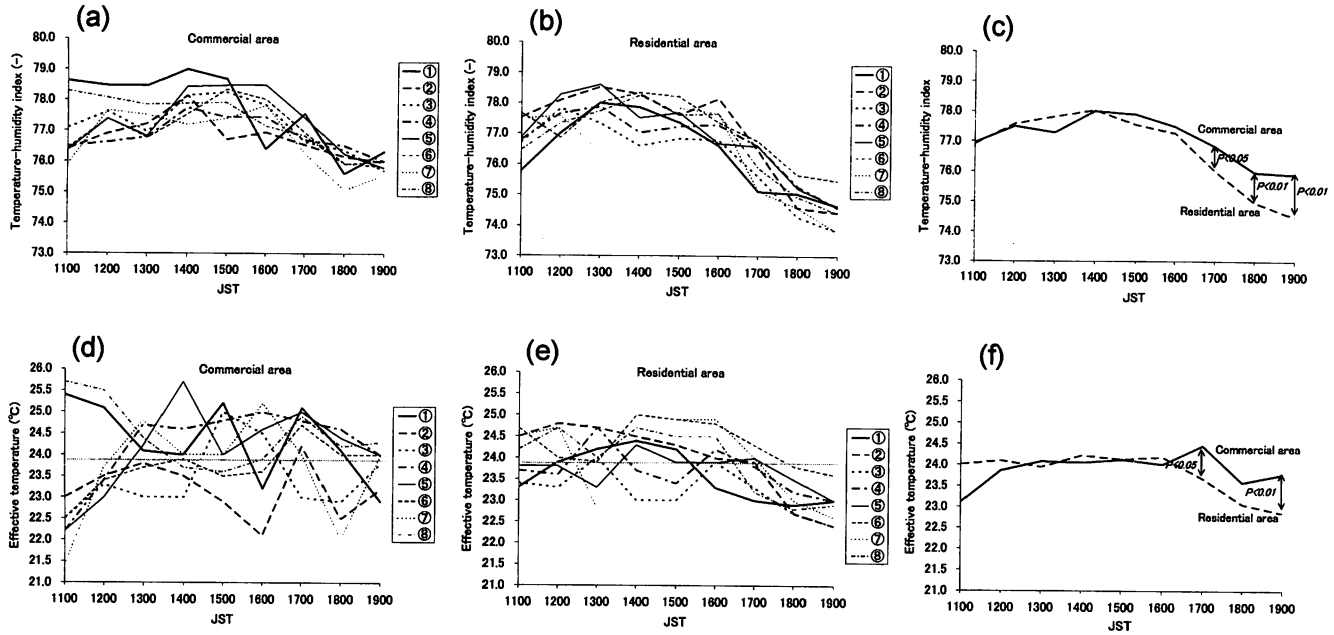

Fig. 6 Same as Fig. 3 but for (a) (b) (c) temperature-humidity index (THI) and (d) (e) (f) effective temperature (ET). The light straight lines in Figs. 6d-6e indicate the boundary value of comfort defined by Ohara (1975).

4. Discussion

4.1 Human discomfort in the CO and RE

The boundary value of comfort defined by ET is represented by the light straight lines in Fig. 6. In Japan, the comfort values of ET are considered within 20.0－24.0 ℃ (Ohara 1975). At 1100－1200 JST, the observation sites of the over-limit ET appear a lots in the RE due to a weak wind in this space as shown in Fig. 5b. Then, after 1700 JST, the CO has many sites of the over-limit ET although there are almost comfortable sites in the RE; this result is similar to the THI that the wind speed is unrelated to a human comfort for both spaces.

Kawahara et al. (1994) proposed a guideline for the heat disorders under taking exercises. They alerted a danger of occurrence of heat disorders when the dry- and wet-bulb temperatures show 28－31 ℃ and 21－24 ℃, respectively, and suggested making every effort to rest. As can be seen in Table 1, although such alert conditions appear at the almost sites of CO until 1600 JST, safe conditions already appear at all sites of RE after 1400 JST (except one site at 1600 JST).

These discomfort conditions in the CO are attributed not to the high air-temperature but to the high absolute-humidity mentioned in the previous section, and bring a danger of heat disorders.

4.2 Water vapor source

We will here consider the water vapor source in the CO. The local water vapor is supplied from the vegetation or water surface (sea, river, and so on). Additionally, the artificial sources of water vapor exist: automobiles and cooling towers. The increase of specific humidity due to anthropogenic latent-heat, including automobiles and cooling towers, is about 0.2 g/kg in the Tokyo metropolitan area which is the greatest city of Japan (Fujibe 2002). Therefore, the specific humidity difference of 1－2 g/kg between the CO and RE, shown in Fig. 4f, is difficult to consider the influence of the anthropogenic latent-heat. Moreover, the traffics measured in the CO were smaller than those in the RE throughout the observation.

Table 1 The number of alert sites in the commercial and residential spaces. The alert conditions are defined as showing 28−31℃ and 21−24 ℃ for dry- and wet-bulb temperatures, respectively, by Kawahara (1994).

JST	The number of alert sites In CO	The number of alert sites In RE
11	2	4
12	7	7
13	4	3
14	7	0
15	7	0
16	5	1
17	2	0
18	1	0
19	0	0

Many natural surfaces such as bare soil and vegetations exist in the RE as can be seen in Fig. 2b. Especially, there are many irrigated rice paddies in the observation period. Although the CO also has the parks and tree-lined streets, many natural sources of water vapor exist in the RE, compared with those in the CO.

Consequently, it is considered that the water-vapor sources within the observation space are poorer in the CO than in the RE. That is, the humid air in the CO is supplied from external areas.

4.3 Effects of sea breeze

Since the CO is located not far from the RE (about 2 km), an influence of the mesoscale meteorological fields on the microscale ones is probably the same almost in both spaces. The sea breeze arrival is judged from a rapid change of the wind speed and direction. This change indicates that the sea breeze from the coast gradually penetrates inland; the sea breeze began to develop at 0900−1000 JST near the coast southeastward from the observation area, and then arrived at the observation areas, 16 km distant from the coast, at 1300−1400 JST. The sea breeze is considered to arrive at the CO and RE, at 1340−1350 JST, with rapid decrease of air temperature.

Table 2 Parameter values used in Eqs 2 and 3 for calculation of the source area (from Schmid 1994).

Parameters		Equation	α_1	α_2	α_3	α_4
a	Stable	Eq. 2	0.773	1.24	0.957	1.25
	Unstable		0.853	1.23	0.441	1.00
e	Stable	Eq. 2	30.4	1.23	2.60	0.452
	Unstable	Eq. 3	40.4	1.22	15.5	−0.548
x_m	Stable	Eq. 2	4.30	1.28	1.74	0.688
	Unstable	Eq. 3	5.37	1.25	5.96	−0.472

This arrival time of sea breeze at inland was consistent with the time of rapid increase of specific humidity in the CO as mentioned in Figs. 4d and 4f. Therefore, it is suggested that the afternoon cold- and humid-air in the CO is supplied by the cool and moist sea-breeze. However, the RE, which is extremely close to the CO, seems to be not influenced by such a sea breeze. We will try to find a reason for this in the following section.

4.4 Estimation of source area

We next consider upwind areas that influence the meteorological fields of the observation sites. Schmid (1994) estimated a *source area*, which influences observation data, with use of the backward trajectory considering effects of the turbulent diffusion. The parameters, D_1 and D_2, of the source area vary with the atmospheric stability:

$$D_1 = z_0 \alpha_1 \left(\frac{z}{z_0}\right)^{\alpha_2} \exp\left(\alpha_3 \left(\frac{z}{L}\right)^{\alpha_4}\right) \qquad (2)$$

and

$$D_2 = z_0 \alpha_1 \left(\frac{z}{z_0}\right)^{\alpha_2} \left(1 - \alpha_3 \frac{z}{L}\right)^{\alpha_4}, \qquad (3)$$

where z_0 is the roughness length, and L the Monin-Obkhov stability length. The symbols α_1, α_2, α_3, and α_4 are listed in Table 2. Although z is the actual observation height, we regard this height as the sea breeze height over the CO canopy layer (i.e., z = 30 m). D_1 in Eq. (2) is equal to a (m)

under stable and unstable conditions, and e (m) and x_m (m) under stable conditions, where a is the distance from the upwind edge of source area to the observation site, e the distance from the downwind edge of source area to the observation site, and x_m the maximum source location from an observation site. By the way, e and x_m under unstable conditions are calculated by use of Eq. (3). Under unstable conditions ($4.0\times10^{-4} \leqq -z/L \leqq 1$), a = 35−56 (31−47) m, e = 551−2553 (473−2192) m, and x_m = 150−376 (127−317) m were calculated for each observation site in the CO where z_0 = 1.0 m (z_0 = 2.0 m) was assumed; under stable conditions ($2.0\times10^{-4} \leqq z/L \leqq 0.1$), a = 52−55 (44−47) m, e = 2107−4495 (1797−4259) m, and x_m = 336−478 (277−393) m were calculated.

On the other hand, for each site in the RE where z_0 = 0.2 m (z_0 = 0.5 m) was assumed, a = 52−81 (42−66) m, e = 785−3637 (642−2973) m, and x_m = 226−563 (179−448) m were calculated under unstable conditions; a = 77−81 (62−65) m, e = 3052−7233 (2472−5858) m, and x_m = 527−750 (408−580) m were calculated under stable conditions. Figure 7 shows the region including the upwind edge to the downwind edge of the source area for each site.

The Pasquill stability classes (Pasquill 1961), at the time when the sea breeze arrived at the two spaces, were estimated at the site A shown in Fig.1. The classes are determined by the shortwave radiation and wind speed. When the sea breeze covered the site A, the Pasquill stability class was B or C (unstable or weak unstable conditions). This implies that the unstable conditions still appear in the sea-breeze stage. That is, the source area shown in Fig.7b, including the A-class river nearby in the CO, is more suitable during the observation period. Consequently, the sea breeze efficiently intends to transport the cold and moist air supplied from the river into the CO space.

In both CO and RE, almost the north-southward and west-eastward streets cross each other as can be seen in Fig. 2. Because the sea breeze with the moist air penetrates northwestward over these spaces, the current direction of the air crosses the street directions. Therefore, the horizontal advection of the moist air transported by the sea breeze, which passes through the street canyon, is small within the CO and RE canopy layers.

Therefore, the moist air is probably mixed downward from the upper atmosphere into the urban canopy layer. Then, a mechanical mixing generated by buildings is more active in the CO than in the RE, because the buildings are taller and denser in the CO. Additionally, the free convection under dense and high buildings is more active than that under coarse and low buildings (Kondo and Ishida 1997).

5. Conclusions

We investigated a formation mechanism of the discomfort conditions, long-continued till the evening, in the commercial space of Okayama City, Japan. As a result, the upper air over the commercial urban canopy layer was mechanically transported to the surface due to denser and taller buildings. Additionally, the surface air-temperature became lower and the absolute humidity became higher, because the cold and moist air originated from the river was transported by the sea breeze. This moist air increased the THI in the commercial space and enhanced a risk of the heat disorder till the evening in this space.

Acknowledgement

The meteorological data were made available by the Japan Meteorological Agency, Okayama Prefectures along with relevant cities. We thank Prof. Osamu Tsukamoto (Okayama University, Japan) for providing the observation data. We also thank Prof. Hitomi Ushioda (Hyogo University of Teacher Education, Japan) for her advice about the temperature-humidity index.

References

Aida M, Yaji M (1979) Observations of atmospheric downward radiation on the Tokyo area. Boundary-Layer Meteor 16: 453−465

Barradas VL (1991) Air temperature and humidity and human comfort index of some city parks of Mexico City. Int J Bio-

meteorol 35: 24-28

Benjamin TB (1968) Gravity currents and related phenomena. J Fluid Mech 31: 209-248

de la Casa AC and Ravelo AC (2003) Assessing temperature and humidity conditions for dairy cattle in Cordoba, Argentina. Int J Biometeorol 48: 6-9

Droegemeier KK, Wilhelmson RB (1987) Numerical simulation of thunderstorm outflow dynamics. Part I : Outflow sensitivity experiments and turbulence dynamics. J Atmos Sci 44: 1180-1210

Fujibe F (2002) Long-term humidity changes on hot days in the central part of Tokyo. Tenki 49: 473-476

Givoni B (1991) Impact of planted areas on urban environmental quality: a review. Atmos Environ B 25: 289-299

Hoshi A, Inaba Y (2005) Meteorological conditions and sports deaths at school in Japan, 1993－1998. Int J Biometeorology 49: 224-231

Kawahara T, Nakai S, Siraki K, Morimoto T, Asayama M (1994) Supohtsu katsudouchu no necchushou yobou gaidobukku, in Japanese: 1-48

Kondo J, Ishida S (1997) Sensible heat flux from the earth's surface under natural convective conditions. J Atmos Sci 54: 498–509

Lemonsu, A, Masson V (2002) Simulation of a summer urban breeze over Paris. Boundary-Layer Meteor 104: 463－490

National Astronomical Observatory (2004) Rika Nenpyo (Chronological Scientific Tables 2004), in Japanese

Ohara J (1975) Hyakumannin no kukichowa, in Japanese: 1-259

Oke, TR (1988) The urban energy balance. Prog Phys Geogr 12: 471－508

Pasquill F (1961) The estimation of the dispersion of windborn material. The Meteor. Magazine 90: 33-49

Saaroni H, Ziv B (2003) The impact of a small lake on heat stress in a Mediterranean urban park: the case of Tel Aviv, Israel. Int J Biometeorol 47: 156-165

Schmid HP (1994) Source areas for scalars and scalar fluxes. Boundary-Layer Metorol 67: 293-318

Somparn P, Gibb MJ, Markvichitr K, Chaiyabutr N, Thummabood S, Vajrabukka C (2004) Analysis of climatic risk for cattle and buffalo production in northeast Thailand. Int J Biometeorol 49: 59-64

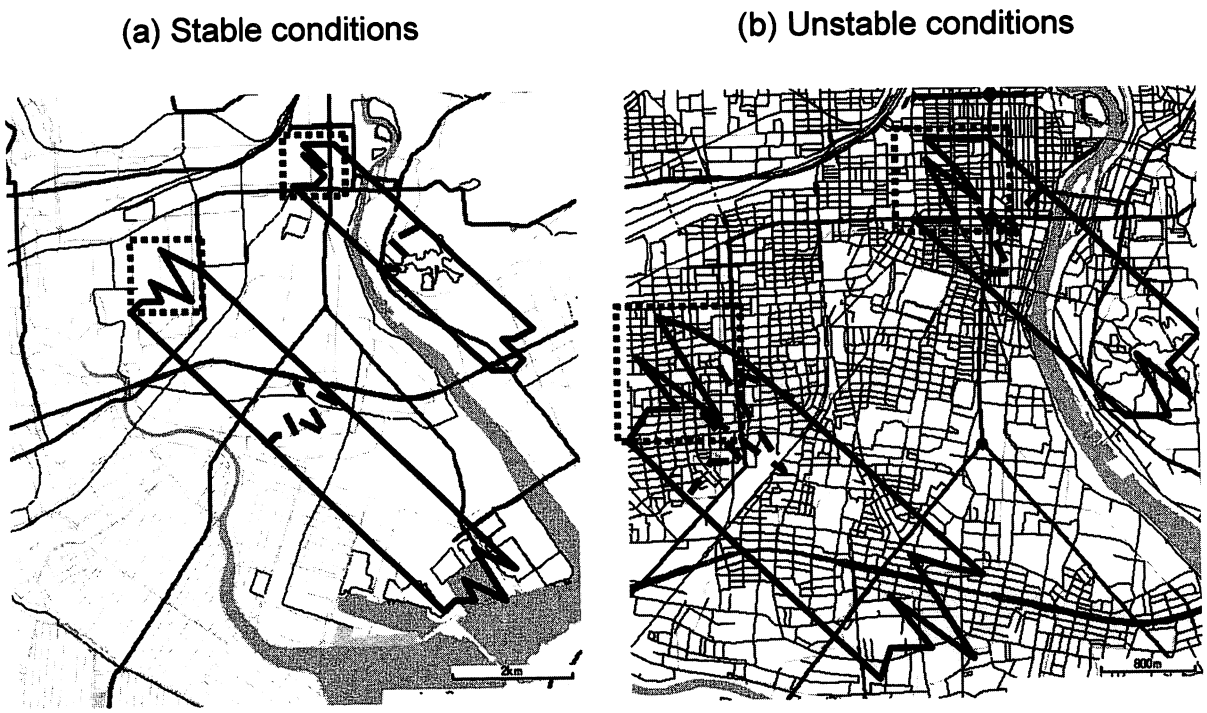

Fig. 7 Regions including the upwind edge to the downwind edge of the source area for each site under (a) stable and (b) unstable conditions in the commercial (z_0 = 1.0 m) and residential (z_0 = 0.2 m) spaces. The solid lines represent the areas connecting the edges of source-area length for z/L = 0.1 in (a) and $-z/L = 4.0\times10^{-4}$ in (b). The dashed lines represent those connecting upward edges of source area for $z/L = 2.0\times10^{-4}$ in (a) and $-z/L$ = 1 in (b).